LAWRENCE
LIVERMORE
NATIONAL
LABORATORY

Conformal Polymer CVD

S. H. Baxamusa

August 14, 2014

Chemical Vapor Deposition Polymers: Fabrication of Organic Surfaces and Devices

Disclaimer

This document was prepared as an account of work sponsored by an agency of the United States government. Neither the United States government nor Lawrence Livermore National Security, LLC, nor any of their employees makes any warranty, expressed or implied, or assumes any legal liability or responsibility for the accuracy, completeness, or usefulness of any information, apparatus, product, or process disclosed, or represents that its use would not infringe privately owned rights. Reference herein to any specific commercial product, process, or service by trade name, trademark, manufacturer, or otherwise does not necessarily constitute or imply its endorsement, recommendation, or favoring by the United States government or Lawrence Livermore National Security, LLC. The views and opinions of authors expressed herein do not necessarily state or reflect those of the United States government or Lawrence Livermore National Security, LLC, and shall not be used for advertising or product endorsement purposes.

Conformal polymer CVD

Salmaan Baxamusa

baxamusa1@llnl.gov, 925-422-0378

Lawrence Livermore National Laboratory, 7000 East Avenue, Livermore CA USA

1.0 Introduction

One of the distinguishing features of vapor-phase deposition is the ability to conformally coat topographically complex substrates. Historically, this has been problematic for polymer coatings because polymer research has focused almost exclusively on liquid-phase synthesis and casting. Polymer vapor deposition technologies such as plasma polymerization, parylene, molecular layer deposition, oCVD, and iCVD allow for conformal polymer coatings that are not accessible through liquid means. This chapter will discuss the fundamental physical mechanisms that govern the conformality of polymer CVD coatings, review the relevant experimental evidence, and finally discuss several applications where conformal CVD polymer coatings have enabled new applications.

1.1 Vapor phase transport

In the vapor phase, reactants diffuse via intermolecular collisions into very small geometries such as pores, trenches, and even the spaces between woven fibers. The mean free path, which is the average distance between intermolecular collisions in the vapor phase, can be engineered over a wide range of length scales because it varies as the inverse of pressure. At atmospheric pressure, the mean free path is only dozens of nanometers, but at typical deposition pressures (~100 mtorr) the mean free path can be nearly a millimeter and at high vacuum the mean free path exceeds a meter. The ratio of the mean free path to the characteristic geometric length scale is known as the Knudsen number (Kn) and is a key parameter in vacuum deposition. When Kn < 1, molecular movement is governed by classical diffusion

which results from the intermolecular collisions. This diffusion allows reactive species to impinge evenly at all surfaces, resulting in conformal deposition. When $Kn > 1$, the flow regime is known as molecular flow. Intermolecular collisions are infrequent in molecular flow and the trajectory of reactive species from its source to the deposition substrate is based on line-of-sight, resulting in non-conformal deposition. This is a common limitation for high-vacuum PVD techniques such as low-pressure sputtering or electron beam PVD. Even at the higher pressures used for CVD, the local Knudsen number can easily exceed unity when coating complex topographies because the relevant length scale can shrink to sub-micron levels.

In practice, this line-of-sight limitation is mitigated because reactant molecules that impinge on the substrate may either stick via irreversible reaction or reflect back into the gas phase, a concept quantified by a parameter called the "sticking probability." When $Kn > 1$, CVD techniques can conformally coat topographically complex substrates if the sticking probability is low enough. An additional factor unique to polymer CVD is that the growing polymer chain is both reactive and has negligible vapor pressure due to its molecular weight. Therefore, reactions between surface-bound molecules are important in polymer vapor deposition, and must be considered in conjunction with gas phase transport when analyzing the factors that govern conformal coverage of the polymer coating.

1.2 Conformal polymer coating applications

The ability to grow conformal polymer coatings directly from vapor-phase reactants make polymer CVD ideal for depositing organic coatings in the interior of high-aspect ratio features. Such features include trenches and overhangs that may be found in integrated circuitry, the narrow and long pores of filtration membranes or microfluidic devices, and complicated topographies of microelectromechanical (MEMS) devices. Lithography or surface patterning also requires conformal deposition within structures defined by the interface between contact masks and the substrate.

Conformal coatings may also be desired for exterior coatings around particles or fibers. Emerging advanced manufacturing techniques such as 3D-printing can be used to fabricate meta-materials with complicated geometries, and polymer coating technologies will eventually be needed for these devices as well. Conceptually, conformal exterior coatings are governed by the same physics and chemistry as interior coatings.

Some applications may require only *qualitatively* conformal coatings; that is, a polymer coating that is continuous around all surfaces but not necessarily of uniform thickness. Examples of these applications requiring qualitatively conformal coatings include surface modification to control surface energy,[1] protective coatings for biosensors or membranes, [2,3] or the introduction of surface chemical moieties for subsequent functionalization .[4] In other applications, it may be important to have *quantitatively* conformal coatings; that is, coatings that must be of uniform thickness on all surfaces. This is particularly important in optical coatings such as dielectric mirrors ,[5] but is also critical for gas permeable or diffusion barrier films and drug-release devices. Because optimizing the conformality requires tradeoffs with other deposition properties – most importantly deposition rate – understanding whether an application requires qualitatively or quantitatively conformal coatings is an important step in designing the deposition process.

1.3 Conformal polymer coating technologies

In liquid phase coating technologies such as spin or dip coating, surface tension effects cause severe coating non-uniformities when the capillary length of the solvent is larger than the length scale of the geometry to be coated.[6] Capillary length is a material property of a solvent that is largely invariant from one solvent to another and is typically on the order of 1 mm. This renders liquid-phase coating unable to evenly coat the ever-shrinking feature sizes of electronic, biomedical, optical, or mechanical devices. Vapor deposition removes the constraints imposed by solvent surface tension.

The deposition of poly(p-xylelene) (known by its trade name parylene) is one of the oldest vapor phase polymerization techniques, having been commercialized by Union Carbide in the 1960s. In parylene deposition, a paracyclophane monomer decomposes into p-xylelene monomer units at high temperatures (~550 $^\circ$C); these monomer units react at the substrate to form the polymer. Parylene coatings are in general found to be conformal.[7] An excellent monograph on the mechanism of parylene deposition is available.[8]

Another major vapor phase polymerization technique is plasma CVD, first popularized in the 1970s. In plasma CVD, a glow discharge decomposes the gaseous monomer into reactive fragments. These reactive fragments recombine at a surface, often through complex and unexpected chemical pathways, to form a polymer film. The presence of non-uniform electric fields and charged species can lead to coating non-uniformities, especially in corners and at edges.[9] The deposition rate of plasma polymers is determined by a balance between concurrent etching and deposition, so any place on the substrate where these relative rates are altered will have non-uniform and non-conformal deposition.[10] Conformal polymer deposition is possible to some degree,[11] although systematic studies to understand the conformality of plasma CVD polymers are limited and this aspect of plasma polymerization remains poorly understood. Conformality of inorganic films deposted via plasma CVD has been considered.[12]

The gold standard in conformal coating is atomic layer deposition (ALD), in which bifunctional precursors are sequentially introduced into a vacuum chamber to form inorganic metal and ceramic coatings. ALD chemistry is essentially a condensation reaction between two precursors, which bears strong resemblance to reaction pathways for step growth polymerization. Indeed, a variant of ALD, termed molecular layer deposition (MLD) was first described in the 1990s and uses organic precursors to grow polymers or inorganic/organic polymer hybrids.[13-15] Because each precursor is reactive only with the other, the reaction is self-limiting and can be used to grow films approximately one molecular layer at a time. MLD is therefore quantitatively conformal in theory, although incomplete exposure of the substrate to the reactant will lead to non-uniformity in film thickness. Models have been developed to

determine the effect of mass transport limitations on the conformality of ALD coatings; these models also apply to MLD.[16,17] One of the limitations of MLD is that deposition rates are slow, on the order of nm/min, but the available material set is growing.

Oxidative chemical vapor deposition (oCVD) is a technique for depositing conducting polymers. Step growth of monomers is achieved with the use of an oxidant, such as an evaporated metal halogen salt or halogen gas. Like other vapor phase processes, oCVD films are conformal over micron scale features.[18] The physical processes governing the conformality of oCVD films have not been studied in detail, but the use of a halogen gas as opposed to an evaporated metal halogen salt has been shown to result in more conformal films. [19]

Finally, initiated chemical vapor deposition (iCVD), a vapor deposition analog of free-radical polymerization, has been used extensively to create conformal coatings.[20,21] The balance of this chapter will focus heavily on iCVD films, as their conformality has been given considerable analytical attention. Many of the concepts discussed in this chapter may be adapted to other polymer CVD mechanisms, and the qualitative conclusions of iCVD studies are broadly applicable to vapor phase polymer deposition. Parallels to parylene deposition, whose kinetics have been studied extensively, will be highlighted in the development of the reaction-diffusion model in Section 3.

Some examples of conformal polymer deposition are shown in Figure 1. Figure 1a shows iCVD, spin-coated, and plasma polymer films inside of trench structures. The iCVD film is conformal around the trench. The non-uniform spin-coated film structure reflects the effect of surface tension in the confined geometry. The plasma polymer is somewhat continuous although the coating is depleted around exterior corners and sidewall coverage is not uniform. Figure 1b is an XPS map demonstrating parylene deposition within the serpentine channels of a microfluidic device. A conformal MLD coating around a nanoparticle is shown in Figure 1c.

2.0 Gas and surface reactions

Polymer CVD involves two key steps: transport of reactants from the vapor phase to the substrate and polymerization which lead to film formation. In general, polymerization occurs at the surface because high molecular weight growing chains have effectively zero vapor pressure. For example, iCVD is a free-radical polymerization process whose rate is determined by the reaction between growing polymer chains and monomer molecules. The rate expression for this process is:[25]

$$rate = k_p C_M \left(\frac{f k_d}{k_t} C_I\right)^{1/2} \qquad\qquad (2.0\text{-}1)$$

Where k_p, k_d, and k_t are kinetic rate constants for propagation, initiator dissociation, and termination respectively; C_M is the monomer concentration; C_I is the initiator concentration, and f is the initiator efficiency. A detailed kinetic and mechanistic study of the iCVD of butyl acrylate shows rate constants that are nearly equal to those for liquid-phase polymerization; growing chain reacts primarily with the liquid-like surface-adsorbed monomer.[26] Parylene deposition proceeds by the reaction of a p-xylelene unit with a surface-adsorbed growing chain.[8]

Surface reactions can occur by one of two mechanisms: the *Langmuir-Hinshelwood* mechanism, where two surface-bound molecules react, or the *Eley-Rideal* mechanism, where a gas phase molecule collides and reacts with a surface-bound molecule. These mechanisms are illustrated in Figure 2. Eley-Rideal is the most likely mechanism for chain initiation, a hypothesis supported by the fact that the time scale for a surface reaction is about a factor of ten longer than the surface lifetime of an adsorbed reactant. Instead, gaseous species likely react directly with a surface-bound molecule, as in the Eley-Rideal mechanism. When this irreversible chemisorption occurs, the reactant is said to "stick" to the surface. This has been observed for both iCVD and parylene deposition. The so-called sticking probability is an important parameter that will be explored in detail in Section 3.

While gas phase transport does not appear explicitly in polymer CVD rate expressions, the supply of reactants to the surface depends wholly upon adsorption from the vapor phase: monomer units must adsorb to the surface at the same rate that they are consumed by polymerization. In the case of iCVD, primary radicals must also appear at the surface to maintain a steady-state of growing polymer chains. Primary radicals are formed by homolysis of the initiator, either thermolytically or photolytically, in the gas phase. In the photolytic case, there is some evidence that radicals may also be formed at the substrate.[27]

Based on the importance of supplying reactants to the surface, it is not surprising that deposition conformality is governed in part by vapor phase processes. In the following section, we will discuss models to understand how to predict and control the conformal deposition of CVD polymers. The interplay between vapor transport and surface reaction is best understood as a balance between supply and consumption. When the supply of reactants to the surface is abundant, then polymerization will take place equally on all surfaces. Where the supply is depleted by consumption of the reactants, the deposition rate will be locally lower.

3.0 The Reaction-diffusion model

3.1 Reaction and diffusion in a pore

A simplified steady-state 1-D reaction-diffusion model of gaseous molecules traveling through a straight circular pore of radius r and length L can be used to understand deposition conformality. In this section, we modify the methods of Asatekin *et al* and Komiyama *et al* to develop a generalized set of governing equations.[2,28] In the absence of gas-phase reactions, the concentration C_i of the ith species can be expressed as:

$$\frac{Dr}{2}\frac{d^2C_i}{dx^2} = v_i \qquad\qquad (3.1\text{-}1)$$

with boundary conditions:

$$C_i|_{x=0} = C_{i,o} \qquad\qquad (3.1\text{-}2)$$

$$D_i\frac{dC_i}{dx}\bigg|_{x=L} = v_i|_{x=L} \qquad\qquad (3.1\text{-}3)$$

where x is the spatial dimension, D_i is the diffusivity, v_i is the local surface flux to the wall of the pore due to reaction, and $C_{i,o}$ is the concentration at the pore entrance. The geometry of the pore and the governing equations and boundary conditions are shown in Figure 3.

Boundary condition (3.1-2) specifies the concentration at the entrance of the pore and the boundary condition and boundary condition (3.1-3) states that the flux of the ith species at the bottom of the pore is equal to the surface flux due to reaction. Note that the classical diffusivity does not apply in this analysis because Kn>1 for CVD in a narrow pore. For molecular flow in a pore, the diffusivity based on kinetic theory is:

$$D_i = \frac{2r}{3}\overline{V_i} \qquad\qquad (3.1\text{-}4)$$

where $\overline{V_i}$ is the mean gas velocity. Analogous expressions valid in different geometries (trenches, square pores, etc.) are available.[29]

We will consider these governing equations in the context of iCVD because there are several experimental results that provide a basis for comparison. Analogous arguments apply for other polymer CVD systems. In iCVD, there are two species of interest in the gas phase: the monomer M and the initiating radical I (the terms initiator and primary radical are also used interchangeably to refer to this species).

The steady-state surface flux v_i has a physical interpretation for the monomer: it is simply the deposition rate because the net amount of monomer that leaves the gas phase incorporates into the growing film. No such interpretation can be made for the initiating radical. Therefore, we adopt the concept of a sticking probability Γ_i, which is the probability that an impinging gas phase molecule irreversibly sticks to the surface. Therefore, the steady-state surface flux is the product of the sticking probability Γ_i with the surface-incident flux N_i.

$$v_i = \Gamma_i N_i = \frac{1}{4} \Gamma_i C_i \overline{V_i} \tag{3.1-5}$$

where we have evaluated N_i using ideal kinetic theory.

Equation (3.1-1) can therefore be rewritten as:

$$\frac{d^2 \psi_i}{d\lambda^2} = \Phi_i^2 \psi_i \tag{3.1-6}$$

where we have introduced the non-dimensional variables $\lambda = x/L$ and $\psi_i = C_i/C_{i,o}$, and grouped parameters into a so-called Thiele modulus Φ_i

$$\Phi_i^2 = \frac{3\Gamma_i}{4} \left(\frac{L}{r}\right)^2 \tag{3.1-7}$$

The Thiele modulus frequently appears in reaction-diffusion problems and is often assumed to be constant. However, the presence of the sticking probability in the Thiele modulus warrants caution in the analysis of both the monomer and the initiator concentration profiles. The sticking probability of the monomer has a clear physical relationship to the surface reaction rate given by Eq (2.0-1):

$$\frac{1}{4} \Gamma_M C_M \overline{V_M} = h_{ml} k_p K C_M \left(\frac{f k_d}{k_t} C_I \right)^{1/2} \qquad (3.1\text{-}8)$$

where we have used the subscripts M and I to denote the monomer and initiator respectively; the monolayer height h_{ml} is used to convert the volumetric rate expression to a surface rate expression; and the adsorption constant K relates the gas phase monomer concentration to the surface concentration. [26] Any appropriate rate expression can be used here to extend this analysis to other systems or polymer deposition reaction mechanism. Eq (3.1-8) states that the net impingement of monomer is equal to the deposition rate, which itself depends upon the concentration of initiator. For the primary radical, the sticking probability has been experimentally verified to depend on the monomer surface concentration. Therefore Eq (3.1-6) must be solved simultaneously for both the monomer and the initiator. When combined with the mixed boundary condition Eq (3.1-3), it becomes clear that this boundary value problem is not amenable to an analytical solution. However, some general observations can be made based on the form of Eq (3.1-6). Eq (3.1-6) has an analytical solution when simplifying assumptions are made; this solution is discussed in Section 3.4

The Thiele modulus represents the ratio of reaction rate to diffusion rate (for the case of the monomer, this can be seen by substituting Eq (3.1-8) and (3.1-4) into (3.1-5)). Systems with a large Thiele modulus are diffusion-limited and those with a low Thiele modulus are reaction-limited. In the limit of low Thiele modulus (i.e., at slow reacation rates), Eq (3.1-6) has the solution $\psi_i = 1$; that is, the concentration does not vary down the length of the pore. This leads to an important general conclusion for the conformality of polymer CVD films: *conformal deposition is preferred when the surface reaction rate (equivalently, the rate of irreversible adsorption onto the surface) is lower than the gas diffusion rate.*

The form of the Thiele modulus also suggests two corollaries: *1) conformal deposition is preferred when the sticking coefficient is low and 2) conformal deposition is hindered when the aspect ratio of the feature is large.* The Thiele modulus captures this competition between sticking probability and aspect ratio.

A common method for evaluating the conformality of films deposited in pores is to measure (e.g., via electron microscopy) the step coverage S, defined as the ratio of the film thickness at the bottom of a feature to the thickness at the top. This is equivalent to the ratio of the deposition rates at the top and the bottom. Based on Eq (2.0-1), the step coverage for a free-radical iCVD system can be written in terms of the non-dimensionalized reactant concentrations:

$$S = \frac{r_b}{r_t} = (\psi_I)^{1/2} \psi_M \big|_{\lambda=1} \qquad\qquad (3.1-9)$$

Again note that any appropriate rate expression can be used here, allowing for adaptability to other kinetic models.

Two limiting cases for the step coverage can be readily identified.

Case 1: $\Phi_M \ll \Phi_I$

When the monomer concentration profile is nearly uniform throughout the pore ($\psi_M \sim 1$) relative to the initiator concentration profile, the step coverage is determined entirely by the initiator. The step coverage is thus $S = (\psi_I)^{1/2}\big|_{\lambda=1}$. This condition occurs when the sticking probability for the monomer is low. Eq (3.1-8) shows that this corresponds to a low polymerization rate (low rate constant k_p, a low rate of initiator homolysis k_d, a low initiator efficiency f, or high termination rate k_t) or when the initiator sticking probability Γ_I is much larger than the monomer sticking probability Γ_M.

Case 2: $\Phi_I \ll \Phi_M$

When the initiator concentration profile is nearly uniform throughout the pore ($\psi_I \sim 1$) relative to the monomer concentration profile, the step coverage is determined entirely by the monomer. The step

coverage is thus $S = \psi_M|_{\lambda=1}$. As opposed to Case 1, this condition is achieved when the polymerization rate is high or when the initiator sticking probability Γ_I is much smaller than the monomer sticking probability Γ_M.

Figure 4 shows numerical solutions to Eq (3.1-6) solved simultaneously for both monomer and initiator. To capture the coupled nature of the concentration profiles, these solutions assume that the monomer sticking probability varies with the square root of the initiator concentration (as in Eq (3.1-8)) and that the initiator sticking probability varies linearly with the monomer concentration. The ratio of sticking probabilities is $\Gamma_M/\Gamma_I = 0.1$, 1, and 10 in the three solutions, corresponding to case 1, the transition between case 1 and case 2, and case 2, respectively. These solutions highlight the importance of the relative magnitudes of the sticking probabilities in determining the step coverage.

Figure 5 shows the step coverage, as defined by Eq (3.1-9), for a variety of sticking probabilities and aspect ratios. In these solutions, the ratio Γ_M/Γ_I was varied. The step coverage decreases with increasing aspect ratio and with increasing initiator sticking probability; the step coverage becomes insensitive to the initiator sticking probability as its value drops below the monomer sticking probability. This represents the transition from case 1 to case 2 described above; when $\Gamma_I < \Gamma_M$, the step coverage is determined entirely by the monomer.

The following sections review several iCVD studies on deposition conformality in the context of the models developed in this section.

3.2 Initiator controlled consumption

The first systematic experiments on the conformality of iCVD coatings studied step coverage inside of trenches.[22] Step coverage was not dependent on gas mean free path, consistent with the fact that Kn>1 inside the trench structures. An analytical model was proposed to connect the number of wall-molecule collisions with the deposition conformality. While this model lacks the rigor of the transport model

developed in Section 3.1, it has intuitive appeal because it is based on a physical mechanism in which reactive species transport down the length of the pore via a wall-collision process.

Consider a reactive molecule that travels down the depth L of the trench with opening width $2r$. It will collide with the wall n times as it travels to the bottom of the trench. If the molecule reacts with the trench wall with sticking probability Γ then the step coverage will be

$$S = (1 - \Gamma)^n \qquad\qquad (3.2\text{-}1)$$

In the original analysis, it was assumed that the deposition rate was proportional to the flux of the reactive molecule. In the case of the initiating radical, the deposition rate is proportional to the square root of its flux (see Eq (2.0-1)), so the exponent n can be replaced by $n/2$. This convention will be adopted here.

The number of collisions n was estimated to be the product of the collision frequency $v_{gas}/(2r)$ and the diffusive time scale L^2/D, where D is the Knudsen diffusivity inside the trench:

$$n = \frac{3}{4}\left(\frac{L}{r}\right)^2 \qquad\qquad (3.2\text{-}2)$$

The prefactor will vary based on the geometry of the trench. Here, we have assumed a straight, cylindrical pore for consistency with section 3.1. This differs from the prefactor used in most experimental studies, which is based on Knudsen diffusion in rectangular trenches of infinite length.

Substituting Eq (3.2-2) into (3.2-1) and assuming $\Gamma\ll 1$ yields

$$\ln(S) = -\frac{3}{8}\Gamma\left(\frac{L}{r}\right)^2 = -\frac{1}{2}\Phi^2 \qquad\qquad (3.2\text{-}3)$$

As in Eq (3.1-6), the Thiele modulus appears as the factor that governs step coverage. Thus, even for a simple approach based on physical intuition, the dependence of the step coverage on the aspect ratio and sticking probability can still be derived.

A number of studies have measured sticking probabilities using Eq (3.2-3) and consistently find $\Gamma = 10^{-2}$–10^{-1} for a variety of deposition conditions and monomer-initiator pairs.[22,30,31] The magnitude of the sticking probability yields a critical insight into the deposition mechanism for iCVD. For typical deposition monomer partial pressures, the sticking probability of the monomer would have to the on the order of 10^{-6} in order to be consistent with the deposition rate. Therefore, experiments that analyze step coverage based on this model fall into Case 1 identified in Sec 3.1: the conformality is initiator consumption controlled. The measured sticking probabilities are thus the sticking probability of the initiator.

The simpler Eq (3.2-3) is in general consistent with numerical solutions of Eq (3.1-6) in commonly encountered experimental regimes. For example, the initiator sticking probability in a trench with aspect ratio $L/r = 10$ and step coverage of 0.86 can be calculated as 0.4×10^{-2} using Eq (3.2-3) and 1.0×10^{-2} using Eq (3.1-6). The agreement is remarkable considering that Eq (3.2-3) was derived using scaling arguments to determine collision frequency and diffusive time scales. The discrepancy may be a resolved through a more accurate estimate of n by, for example, accounting for the reflection mechanism (specular, diffuse, cosine) of the impinging primary radical. Nevertheless, sticking probabilities utilizing Eq (3.2-3) should be considered accurate to within experimental uncertainty.

3.3 Factors affecting the initiator sticking probability

Several iCVD studies have reported the effect of deposition conditions on the initiator sticking probability. Such studies are best understood within the context of the Eley-Rideal mechanism: the sticking probability of the initiating radical increases as the probability of irreversible reaction with a surface-bound monomer increases.

Classical adsorption theory (as might be used in catalysis) predicts that the sticking probability of a species will decrease as the surface becomes more heavily populated by adsorbed molecules. This is due to Langmuir-type adsorption occupying the surface sites that accommodate the impinging species. In

iCVD higher monomer surface coverage actually promotes irreversible adsorption of the primary radical because it increases the probability that an impinging primary radical strikes and reacts with a monomer.[22] This deviation from classical adsorption theory makes it clear that the monomer serves as the adsorption site for the primary radical.

From a practical perspective, monomer surface coverage is easily controlled by changing the partial pressure of the monomer gas during deposition through a combination of deposition pressure, substrate temperature, and monomer flowrate. The fractional saturation of the monomer gas, P/P^{sat} is the relevant normalized parameter and is the primary process variable used to tune film conformality. A low initiator sticking probability, and therefore a high degree of conformality, can be achieved by operating under conditions where $P/P^{sat} < 0.1$. Figure 6 demonstrates control over step coverage within trenches by varying P/P^{sat}.

This can be generalized to other polymer CVD systems: *whenever a reactive molecule adsorbs by irreversible chemical reaction with a surface species, a low coverage of the surface species will enhance deposition conformality*. The chief drawback of operating under these conditions is that the deposition rate is slower.

The reactivity of the monomer affects the initiator sticking probability as well. For similar values of P/P^{sat}, a divinyl acrylate monomer was found to have a greater sticking probability than a monovinyl methacrylate monomer, suggesting that the increased vinyl concentration or the increased steric accessibility of the acrylate (or both) is responsible for the enhanced sticking of the primary radical. Additional evidence for the Eley-Rideal mechanism in iCVD was provided in that study by showing that the substrate temperature, when holding the fractional saturation constant, does not affect the sticking probability. Thermally-activated surface diffusion or reaction therefore does not play an important role in the deposition mechanism.[30]

An analogy can be drawn between the parylene monomer and the initiating radical in iCVD, as both serve as the reactive impinging species in their respective depositions; In parylene deposition, an impinging reactant will only stick to the surface if it impinges directly on and reacts with a reactive chain end.[8] The sticking probability has been reported to vary between 10^{-5} and 10^{-3} at high and low substrate temperatures, respectively. If thermally activated surface processes (such as reaction) were important, the sticking probability would increase, not decrease, with temperature.

The most common initiating radical for iCVD is a *tert*-butoxy radical, and the studies cited in this section invariably utilized this initiator. When the initiating radical was instead a mixture of oxybenzoate and *tert*-butoxy radicals, the sticking probability was found to increase by a factor of three. One possibility is that the sticking probability of a primary radical is affected by vapor pressure; oxybenzoate is considerably heavier than *tert*-butoxy. It is also larger, and so its physical cross section – the surface area sampled by the primary radical – during impingement may also play a role. Yet another possibility is that the oxybenzoate is simply more reactive and is therefore more likely to initiate a growing polymer chain upon impingement.[31]

3.4 Monomer controlled consumption

Most iCVD sticking probability measurements have been performed on trench structures with aspect ratios less than 10. These studies have invariably been performed in systems where the conformality is controlled by initiator consumption, i.e., the sticking probability of the initiator is much larger than that of the monomer. There are several reports of iCVD inside of pores with aspect ratios of over 100 which appear to be monomer-consumption controlled.[2,32,33] Asatekin *et al* developed a reaction-diffusion transport model for the monomer similar to the one developed in Section 3.1. By neglecting the coupled behavior with the initiator and assuming zero flux of monomer at the bottom of the pore, an analytical solution for the monomer concentration profile was obtained:

$$\psi_M = \frac{e^{\Phi_M \lambda} + e^{\Phi_M (2-\lambda)}}{1 + e^{2\Phi_M}} \qquad\qquad (3.4\text{-}1)$$

The zero-flux boundary condition is equivalent to setting the right-hand side of Eq (3.1-3) to zero and is accurate when the sticking probability is small, as is the case for the monomer.

In these systems, the Thiele modulus for the monomer was larger, by about a factor of ten, than that of the initiator.[2] Eq (3.1-7) can be used to estimate the monomer sticking probability as approximately 10^{-6}, in line with estimates in other studies. However, the initiator sticking probability was approximately 10^{-7}, far lower than those measured in low aspect ratio trench structures for the same monomer-initiator system ($\sim 10^{-2}$).[30] Therefore, there are systems in which simultaneous monomer and initiator consumption are important. The reason for the dramatic decrease in initiator sticking probability is unclear. One explanation is that the initiator sticking probability depends upon the aspect ratio of the pore, although there is no known physical mechanism linking the two. Figure 7, from a different study on a similar system, shows electron microprobe analysis of the fluorine content obtained through the cross-section of a membrane coated with fluoropolymer. The presence of fluorine at both the top and bottom of the membrane pore shows successful deposition within these high aspect ratio features.

3.5 Other polymer CVD systems

Conformal films are the result of processing conditions where the surface reaction, rather than vapor phase transport, is the rate-limiting step. For iCVD and parylene deposition, the key is to operate under conditions where the sticking probabilities of the reactants are low. Other polymer CVD systems can be understood in the same way.

The conformality of conducting polymers deposited by oCVD may be controlled by the sticking probability of the oxidant. Bromine gas oxidant results in more conformal films than evaporated $FeCl_3$ oxidant. The sticking probability of bromine gas is likely much lower than the evaporated metal salt due to its considerably higher volatility,[19] consistent with iCVD studies showing decreased conformality when the volatility of the initiating radical is lowered.[31]

The general conclusion that conformality is enhanced when vapor phase transport is not a limiting process is also observed in MLD. A useful chemical processing analogy between CVD and MLD is that the former resembles a continuous process where *rates* are important and the latter resembles a batch process where *durations* are important. Consistent with this analogy, ALD models predict that step coverage is a strong function of *total* exposure time of reactants due to the time required to diffuse reactants into small pores.[16] This has been observed experimentally in MLD systems. [34]

Conformality of plasma CVD is not well understood, but the species formed by fragmentation of organic gases in plasma CVD are thought to be highly reactive. Within the context of sticking probability, these molecular fragments are likely to have very high sticking probabilities and therefore conformal plasma polymer films are difficult to achieve.

A summary of experimental results for a variety of systems is presented in Table 1.

System	Parameter	Effect	Ref
iCVD	P/P^{sat} of monomer near substrate	Increasing P/P^{sat} decreases sticking probability	[22,30]
iCVD	Monomer reactivity	Increased reactivity decreases sticking probability	[30]
iCVD	Mean free path	No effect	[22]
iCVD	Substrate temperature	No effect (when P/P^{sat} held constant)	[30]
Parylene	Substrate temperature	Increased substrate temperature decreases sticking probability. Fractional saturation not controlled.	[7]
oCVD, iCVD	Reactant volatility	Increased volatility of initiator (iCVD) or oxidant (oCVD) decreases sticking probability.	[19]
MLD	Exposure (product of pressure and time)	Step coverage increases with increasing exposure during reaction cycles	[34]

Table 1: Summary of experimental results on factors affecting polymer CVD conformality

4.0 Applications

Conformal polymer CVD is a key part of a number of applications reported in the literature. This section is not an exhaustive list of such applications, but rather highlights the growing number of fields in which the conformality of polymer CVD films contributes or even enables applications. Several of these applications are the subject of more detailed discussion in chapter **[X]**.

The quantitative understanding of polymer CVD conformality is based on deposition inside of well-defined trenches and pores. Direct application of these concepts can be made to patterning of surfaces and deposition inside of membranes.

Contact masks used for surface patterning resemble low aspect ratio trenches. For example, dual-polymer patterned surfaces can be fabricated via iCVD using commercial TEM grids as a contact mask. Because the mask has a finite thickness, the unmasked regions reside at the bottom of a trench whose width is the opening of the mask (7.5-15 μm) and whose depth is the thickness of the mask (~15 μm).[35] Colloids can also be used as contact masks for patterning; the interstitial spaces between colloidal particles as small as 1 μm serve as openings through which reactants must diffuse to reach the surface.[36] The film thickness in the unmasked regions cannot be measured *in situ*, so a witness substrate must be used to monitor film thickness. By operating under conditions that yield high step coverage, the film thickness on the witness serves as a suitable surrogate for the thickness within the mask. Surface patterns can thus be fabricated with *in situ* thickness control. These techniques can be easily adapted to macroscopically curved substrates. Polymer patterns with features sizes as small as 15 μm have been demonstrated on 3-mm diameter rods.[37]

Membranes play a central role in separations technologies for water purification and gas separations. Conformal polymer CVD makes it possible to modify membrane surfaces throughout pores, which can have openings <100 nm and aspect ratios exceeding 1000:1. Fluorinated iCVD coatings deposited on membranes with an 80:1 aspect ratio showed step coverage of approximately 50% even without

optimizing the fractional saturation of monomer.[32] The detailed reaction-diffusion model from Sec 3.4 was used to analyze coverage in 1000:1 aspect ratio pores in track-etched polycarbonate membranes. Conformal hydrophobic coatings in these membranes were shown to enhance the selective diffusion of a hydrophobic molecule relative to a hydrophilic analog.[2]

Conformal deposition to completely fill the inside of high-aspect ratio pores has also been used template the fabrication of cylindrical polymer microstructures. If the coating preferentially deposits at the mouth of the pore, then the opening will eventually pinch off and block the diffusion of reactants into the pore, limiting the growth of the polymer cylinder. Therefore, these templated structures are only accessible when deposition conditions result in conformal coatings.[33] Within mesoporous materials with irregular pore structure, MLD is an attractive technique for depositing polymers. Oxidation of highly conformal MLD films deposited within mesoporous zeolite forms zeolite-supported nanoporous networks that enhance the selectivity of gas separation of H_2 from N_2 by a factor of 100 as compared to uncoated zeolite.[38]

In addition to templating structures, pore-filling via polymer CVD is an important end to itself. Ceramic moisture barrier layers frequently fail due to water permeation through pinholes with diameters ranging between 1-1000 nm. Adsorption isotherms show that cyclic siloxane monomers can adsorb within these pinholes, suggesting that iCVD may be an effective means for healing defects in ceramic water-barrier layers.[39]   Defect planarization, which is closely related to pore-filling, has been demonstrated with cylic siloxane iCVD polymers deposited using a plasma-assisted process.[40] Gap-filling and planarization of micron-sized trench structures for electrical applications is also possible using parylene deposition.[41]

Polymer deposition on non-planar substrates has found application in miniature devices requiring surface modification.   Figure 8a shows a cantilever structure coated with a reactive iCVD polymer that was used

to create a chemical sensor: the film stress induced by the reaction between the polymer coating and an analyte transduced the chemical signal into a mechanical signal via bending of the cantilever.[42]

Several studies have used polymer CVD to modify microfluidic devices. Parylene derivatives were used to modify assembled devices with a channel opening of 75 μm x 100 μm and channel lengths of up to 2.8 mm. In analogy with step coverage, the ratio of the film thickness within the microfluidic channel to the film thickness outside the channel ranged from ~1% to up to 89%. Better coverage was observed for parylene derivatized with lighter side groups, suggesting that the sticking probability increased when the vapor pressure of the precursor was low – or, equivalently, when the fractional saturation was high. These results are consistent with the systematic studies discussed in Section 3 of this chapter. Biotin could be subsequently immobilized on the reactive parylene coatings.[23]

Coating microfluidic devices prior to assembly has enabled new device bonding techniques. The standard technique is to activate poly(dimethylsiloxane) (PDMS) and glass surfaces using oxygen plasma and then to immediately place the surfaces into contact. The PDMS surface is typically patterned with the microfluidic channel topography while the glass surface is flat. By coating the PDMS with an epoxy-containing polymer and coating the glass with an amine-containing polymer, the surface of each piece contains one part of a two-part glue. The bonding proceeds by assembly and subsequent reaction between epoxy and amine. Conformal deposition on the patterned substrate is important for producing a continuous bond between the two pieces and for maintaining the fidelity of the channel geometry. In Figure 8b, such a scheme has been used to assemble devices with channels as thin as 200 nm.[43] Utilizing coatings as opposed to traditional plasma-based bonding also allows non-PDMS microfluidic devices can be bonded. Such bonds display good hydrolytic stability and can withstand over 150 psi without failing.[44,45]

While most analytical work on polymer CVD has been performed on interior coatings in trenches and pores, exterior coatings around masses of particles and fibers are a key area of interest. Powder beds and

fiber mats can be thought of a collection of non-planar substrates with tortuous channels defined by the interstices between the individual particles and fibers; therefore, deposition conditions which yield conformal films are required to coat such substrates.

For particles, agitation is often required because of contact shadowing at the point where particles touch each other or the deposition stage. Rotating iCVD reactors have been designed to aid the agitation process.[46] Microspheres (1-100 μm) have been coated via iCVD [3,46] including the encapsulation of 25 μm drug particles with enteric coatings.[47] Smaller nanoparticles, including carbon nanotubes, have been coated via iCVD as well.[46] MLD can coat nanoparticles smaller than 100 nm, including particles as small as 7 nm.[34,48]

Plasma polymerization has been used to coat individual fibers with acetaldehyde-derived polymer films for cell-adhesion purposes.[49] Similar results were achieved using iCVD to coat wires with an electrically passivating polymer as shown in Figure 8c.[50] However, fibers wound into tows were not evenly coated in a plasma polymerization process due to shadowing effects.[51] This is consistent with the observed conformality plasma polymers (see, for example, Figure 1a). Wound or woven fiber mats are an important class of substrate because the ability to coat commercial textiles enables applications in self-cleaning and sterile consumer products. Polymer-textile systems exhibiting superhydrophobicity and anti-microbial activity have been demonstrated by iCVD.[52,53] Figure 8d shows a cross-section of a fiber from a woven fabric coated with an anti-microbial polymer.

5.0 Conclusion

Polymer CVD technologies enable conformal coatings of complex topographies that have feature sizes ranging from nanometers to millimeters. Liquid-phase coatings are unable to produce conformal coatings on these size scales due to the effects of solvent surface tension. In polymer CVD, conformal coatings result when vapor phase reactants transport evenly to all surfaces of the substrate. This transport occurs in competition with the surface reaction and conformality is best achieved when the surface reaction rate is lower than the gas diffusion rate, a concept embodied by the Thiele modulus. For reaction and diffusion in a pore, the Thiele modulus depends on the sticking probability of the reactant and the aspect ratio of the pore. Systems with a low Thiele modulus – that is, systems with low sticking probabilities and small aspect ratios –result in more conformal coatings. A number of chemical and physical factors have been found to control the sticking probability, which can be quantitatively estimated based on reaction-diffusion models. Conformal polymer coatings via plasma polymerization, parylene deposition, iCVD, oCVD, and MLD are central to a number of applications demonstrated in the literature.

Acknowledgment

References

1. Chu, K.-H., Xiao, R., and Wang, E. N., "Uni-directional liquid spreading on asymmetric nanostructured surfaces," *Nat Mater* **9,** 413 (2010).
2. Asatekin, A. and Gleason, K. K., "Polymeric Nanopore Membranes for Hydrophobicity-Based Separations by Conformal Initiated Chemical Vapor Deposition," *Nano Lett.* **11,** 677 (2011).
3. Baxamusa, S. H., Montero, L., Dubach, J. M., Clark, H. A., Borros, S., and Gleason, K. K., "Protection of Sensors for Biological Applications by Photoinitiated Chemical Vapor Deposition of Hydrogel Thin Films," *Biomacromolecules* **9,** 2857 (2008).
4. Montero, L., Baxamusa, S. H., Borros, S., and Gleason, K. K., "Thin Hydrogel Films With Nanoconfined Surface Reactivity by Photoinitiated Chemical Vapor Deposition," *Chem. Mater.* **21,** 399 (2008).
5. Karaman, M., Kooi, S. E., and Gleason, K. K., "Vapor Deposition of Hybrid Organic–Inorganic Dielectric Bragg Mirrors having Rapid and Reversibly Tunable Optical Reflectance," *Chem. Mater.* **20,** 2262 (2008).
6. Stillwagon, L. E., Larson, R. G., and Taylor, G. N., "Planarization of Substrate Topography by Spin Coating," *J. Electrochem. Soc.* **134,** 2030 (1987).
7. Fortin, J. B. and Lu, T. M., "A Model for the Chemical Vapor Deposition of Poly(para-xylylene) (Parylene) Thin Films," *Chem. Mater.* **14,** 1945 (2002).
8. Fortin, J. B. and Lu, T. M., *Chemical Vapor Deposition Polymerization: The Growth and Properties of Parylene Thin Films* (Springer, 2003).
9. Macak, E. B., Münz, W.-D., and Rodenburg, J. M., "Plasma–surface interaction at sharp edges and corners during ion-assisted physical vapor deposition. Part I: Edge-related effects and their influence on coating morphology and composition," *J. Appl. Phys.* **94,** 2829 (2003).
10. Yasuda, H., *Plasma polymerization* (Academic Press, 1985).
11. Yeo, L. P., Yan, Y. H., Lam, Y. C., and Chan-Park, M. B., "Design of Experiment for Optimization of Plasma-Polymerized Octafluorocyclobutane Coating on Very High Aspect Ratio Silicon Molds," *Langmuir* **22,** 10196 (2006).
12. Fridman, A., *Plasma Chemistry* (Cambridge University Press, 2008).
13. Du, Y. and George, S. M., "Molecular Layer Deposition of Nylon 66 Films Examined Using in Situ FTIR Spectroscopy," *The Journal of Physical Chemistry C* **111,** 8509 (2007).
14. Yoshimura, T., Tatsuura, S., and Sotoyama, W., "Polymer-films formed with monolayer growth steps by molecular layer deposition," *Appl. Phys. Lett.* **59,** 482 (1991).
15. Zhou, H. and Bent, S. F., "Fabrication of organic interfacial layers by molecular layer deposition: Present status and future opportunities," *Journal of Vacuum Science & Technology A* **31** (2013).
16. Gordon, R. G., Hausmann, D., Kim, E., and Shepard, J., "A Kinetic Model for Step Coverage by Atomic Layer Deposition in Narrow Holes or Trenches," *Chem. Vap. Deposition* **9,** 73 (2003).
17. Ja-Yong, K., Ji-Hoon, A., Sang-Won, K., and Jin-Hyock, K., "Step coverage modeling of thin films in atomic layer deposition," *J. Appl. Phys.* **101,** 73502 (2007).
18. Im, S. G., Kusters, D., Choi, W., Baxamusa, S. H., de Sanden, M. C. M. v., and Gleason, K. K., "Conformal coverage of poly(3,4-ethylenedioxythiophene) films with tunable nanoporosity via oxidative chemical vapor deposition," *ACS Nano* **2,** 1959 (2008).
19. Chelawat, H., Vaddiraju, S., and Gleason, K., "Conformal, Conducting Poly(3,4-ethylenedioxythiophene) Thin Films Deposited Using Bromine as the Oxidant in a Completely Dry Oxidative Chemical Vapor Deposition Process," *Chem. Mater.* **22,** 2864 (2010).
20. Alf, M. E., Asatekin, A., Barr, M. C., Baxamusa, S. H., Chelawat, H., Ozaydin-Ince, G., Petruczok, C. D., Sreenivasan, R., Tenhaeff, W. E., Trujillo, N. J., Vaddiraju, S., Xu, J., and Gleason, K. K., "Chemical Vapor Deposition of Conformal, Functional, and Responsive Polymer Films," *Adv. Mater.* **22,** 1993 (2010).

21. Baxamusa, S. H., Im, S. G., and Gleason, K. K., "Initiated and oxidative chemical vapor deposition: a scalable method for conformal and functional polymer films on real substrates," *PCCP* **11,** 5227 (2009).
22. Baxamusa, S. H. and Gleason, K. K., "Thin Polymer Films with High Step Coverage in Microtrenches by Initiated CVD," *Chem. Vap. Deposition* **14,** 313 (2008).
23. Chen, H.-Y., Elkasabi, Y., and Lahann, J., "Surface Modification of Confined Microgeometries via Vapor-Deposited Polymer Coatings," *J. Am. Chem. Soc.* **128,** 374 (2005).
24. Dameron, A. A., Seghete, D., Burton, B. B., Davidson, S. D., Cavanagh, A. S., Bertrand, J. A., and George, S. M., "Molecular Layer Deposition of Alucone Polymer Films Using Trimethylaluminum and Ethylene Glycol," *Chem. Mater.* **20,** 3315 (2008).
25. Odian, G., *Principles of Polymerization* (Wiley, 2004).
26. Lau, K. K. S. and Gleason, K. K., "Initiated Chemical Vapor Deposition (iCVD) of Poly(alkyl acrylates): A Kinetic Model," *Macromolecules* **39,** 3695 (2006).
27. Suresh, A., Anastasio, D., and Burkey, D. D., "Potential of Hexyl Acrylate Monomer as an Initiator in Photo-initiated CVD," *Chem. Vap. Deposition* **20,** 5 (2014).
28. Komiyama, H., Shimogaki, Y., and Egashira, Y., "Chemical reaction engineering in the design of CVD reactors," *Chem. Eng. Sci.* **54,** 1941 (1999).
29. Ohring, M., *Materials Science of Thin Films* (Elsevier Science, 2001).
30. Ozaydin-Ince, G. and Gleason, K. K., "Tunable Conformality of Polymer Coatings on High Aspect Ratio Features," *Chem. Vap. Deposition* **16,** 100 (2010).
31. Xu, J. and Gleason, K. K., "Conformal Polymeric Thin Films by Low-Temperature Rapid Initiated Chemical Vapor Deposition (iCVD) Using tert-Butyl Peroxybenzoate as an Initiator," *ACS Applied Materials & Interfaces* **3,** 2410 (2011).
32. Gupta, M., Kapur, V., Pinkerton, N. M., and Gleason, K. K., "Initiated Chemical Vapor Deposition (iCVD) of Conformal Polymeric Nanocoatings for the Surface Modification of High-Aspect-Ratio Pores," *Chem. Mater.* **20,** 1646 (2008).
33. Ozaydin-Ince, G., Dubach, J. M., Gleason, K. K., and Clark, H. A., "Microworm optode sensors limit particle diffusion to enable in vivo measurements," *Proc. Natl. Acad. Sci. U.S.A.* **108,** 2656 (2011).
34. Loscutoff, P. W., Lee, H.-B.-R., and Bent, S. F., "Deposition of Ultrathin Polythiourea Films by Molecular Layer Deposition," *Chem. Mater.* **22,** 5563 (2010).
35. Baxamusa, S. H., Montero, L., Borrós, S., and Gleason, K. K., "Self-Aligned Micropatterns of Bifunctional Polymer Surfaces with Independent Chemical and Topographical Contrast," *Macromol. Rapid Commun.* **31,** 735 (2010).
36. Trujillo, N. J., Baxamusa, S. H., and Gleason, K. K., "Grafted Functional Polymer Nanostructures Patterned Bottom-Up by Colloidal Lithography and Initiated Chemical Vapor Deposition (iCVD)," *Chem. Mater.* **21,** 742 (2009).
37. Petruczok, C. D. and Gleason, K. K., "Initiated Chemical Vapor Deposition-Based Method for Patterning Polymer and Metal Microstructures on Curved Substrates," *Adv. Mater.* **24,** 6445 (2012).
38. Yu, M., Funke, H. H., Noble, R. D., and Falconer, J. L., "H_2 Separation Using Defect-Free, Inorganic Composite Membranes," *J. Am. Chem. Soc.* **133,** 1748 (2011).
39. Aresta, G., Palmans, J., van de Sanden, M. C. M., and Creatore, M., "Evidence of the filling of nano-porosity in SiO_2-like layers by an initiated-CVD monomer," *Microporous Mesoporous Mater.* **151,** 434 (2012).
40. Coclite, A. M. and Gleason, K. K., "Global and local planarization of surface roughness by chemical vapor deposition of organosilicon polymer for barrier applications," *J. Appl. Phys.* **111** (2012).
41. Zhang, X., Dabral, S., Howard, B. J., Bica, J., Chiang, C., Ochoa, V., Ficalora, P. J., Steinbruchel, C. O., Bakhru, H., Lu, T.-M., and McDonald, J. F., "Parylene as a conformal insulator for submicron multilayer interconnection," *Proceedings of the SPIE* **1805,** 30 (1993).

42. Arora, W. J., Tenhaeff, W. E., Gleason, K. K., and Barbastathis, G., "Integration of Reactive Polymeric Nanofilms Into a Low-Power Electromechanical Switch for Selective Chemical Sensing," *Journal of Microelectromechanical Systems* **18,** 97 (2009).

43. Im, S. G., Bong, K. W., Lee, C.-H., Doyle, P. S., and Gleason, K. K., "A conformal nano-adhesive via initiated chemical vapor deposition for microfluidic devices," *Lab on a Chip* **9,** 411 (2009).

44. Bong, K. W., Xu, J., Kim, J.-H., Chapin, S. C., Strano, M. S., Gleason, K. K., and Doyle, P. S., "Non-polydimethylsiloxane devices for oxygen-free flow lithography," *Nature Communications* **3** (2012).

45. Xu, J. and Gleason, K. K., "Conformal, Amine-Functionalized Thin Films by Initiated Chemical Vapor Deposition (iCVD) for Hydrolytically Stable Microfluidic Devices," *Chem. Mater.* **22,** 1732 (2010).

46. Lau, K. K. S. and Gleason, K. K., "Particle Surface Design using an All-Dry Encapsulation Method," *Adv. Mater.* **18,** 1972 (2006).

47. Lau, K. K. S. and Gleason, K. K., "All-Dry Synthesis and Coating of Methacrylic Acid Copolymers for Controlled Release," *Macromol. Biosci.* **7,** 429 (2007).

48. Bent, S., Loscutoff, P. W., and Clendenning, S., "Fabrication of Organic Thin Films for Copper Diffusion Barrier Layers Using Molecular Layer Deposition," *MRS Online Proceedings Library* **1249** (2010).

49. Hadjizadeh, A., "Acetaldehyde plasma polymer-coated PET fibers for endothelial cell patterning: Chemical, topographical, and biological analysis," *Journal of Biomedical Materials Research Part B: Applied Biomaterials* **94B,** 11 (2010).

50. O'Shaughnessy, W. S., Murthy, S. K., Edell, D. J., and Gleason, K. K., "Stable Biopassive Insulation Synthesized by Initiated Chemical Vapor Deposition of Poly(1,3,5-trivinyltrimethylcyclotrisiloxane)," *Biomacromolecules* **8,** 2564 (2007).

51. Pittman Jr, C. U., Jiang, W., He, G. R., and Gardner, S. D., "Oxygen plasma and isobutylene plasma treatments of carbon fibers: Determination of surface functionality and effects on composite properties," *Carbon* **36,** 25 (1998).

52. Ma, M., Gupta, M., Li, Z., Zhai, L., Gleason, K. K., Cohen, R. E., Rubner, M. F., and Rutledge, G. C., "Decorated Electrospun Fibers Exhibiting Superhydrophobicity," *Adv. Mater.* **19,** 255 (2007).

53. Martin, T. P., Kooi, S. E., Chang, S. H., Sedransk, K. L., and Gleason, K. K., "Initiated chemical vapor deposition of antimicrobial polymer coatings," *Biomaterials* **28,** 909 (2007).
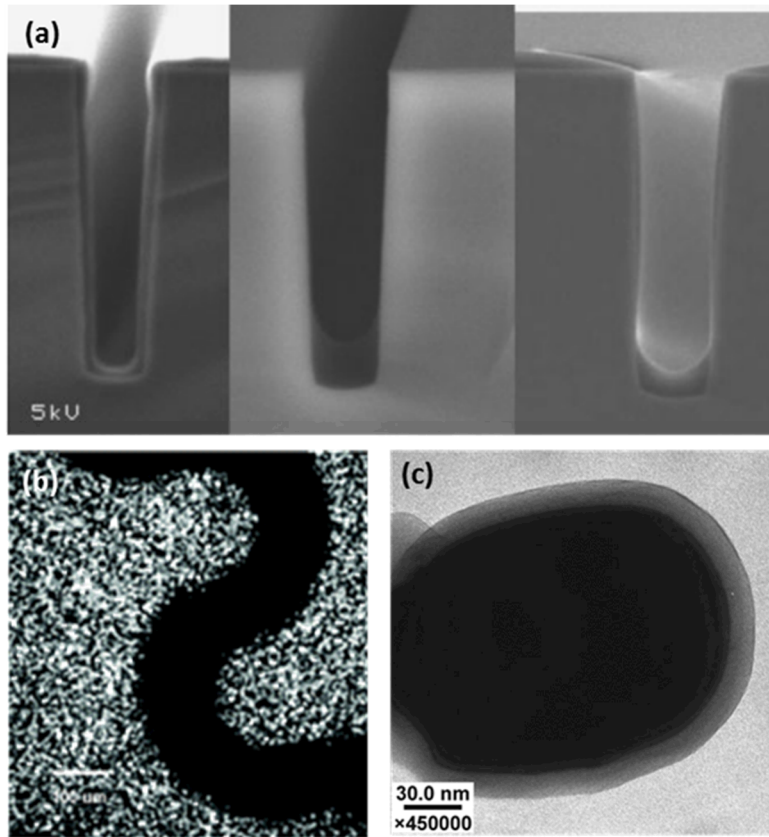
Figure captions

FIGURE 1: (a) polymer coating in trench structures (approximately 2 μm wide by 7 μm deep) deposited via (left to right) iCVD, spin-coating, and plasma polymerization. (b) XPS map of Si showing no silicon within a 100 μm width serpentine microfluidic channel coated with parylene. (c) MLD coating of conformal around a nanoparticle. Reprinted with permission from (a) [22], copyright 2008 Wiley (b) [23], copyright 2005 American Chemical Society (c) [24], copyright 2008 American Chemical Society.
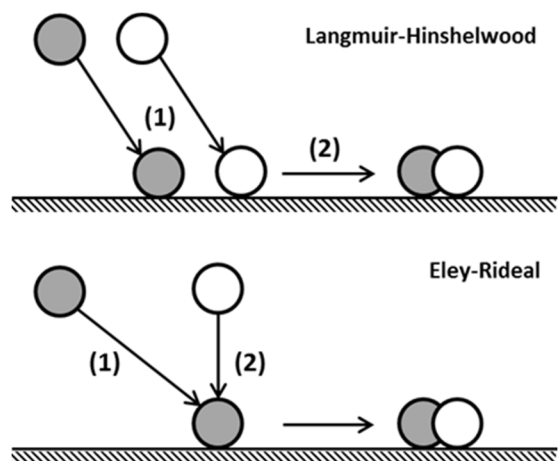
FIGURE 2: Two modes of bimolecular surface reactions. In the Langmuir-Hinshelwood mechanism, the reactants separately adsorb to the surface (1) followed by a reaction between the adsorbed species (2). In the Eley-Rideal mechanism, the first reactant adsorbs to the surface (1), followed by a reaction between the gaseous second species and the adsorbed first species (2).
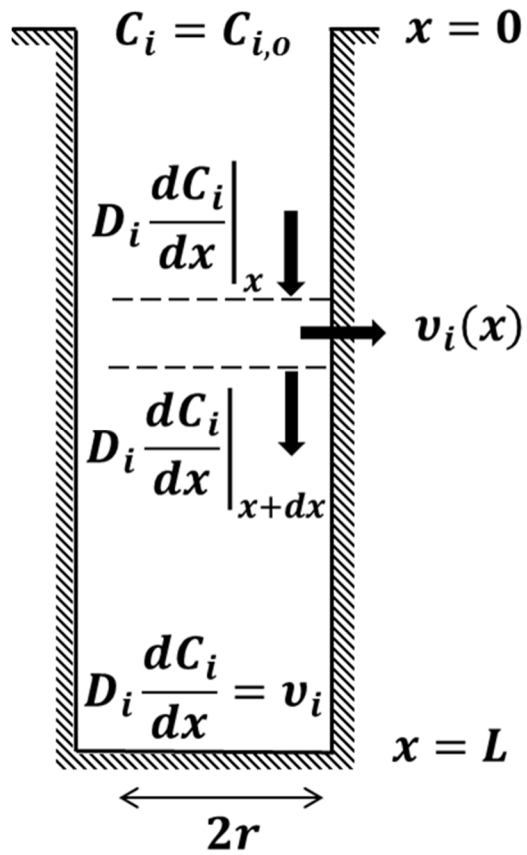
FIGURE 3: Schematic for reaction and diffusion in a pore of radius r and depth L. The boundary conditions at the top (Eq (3.1-2)) and bottom (Eq (3.1-3)) of the pore are shown, and the governing equation (Eq (3.1-1)) is based on a species balance on the differential slice.
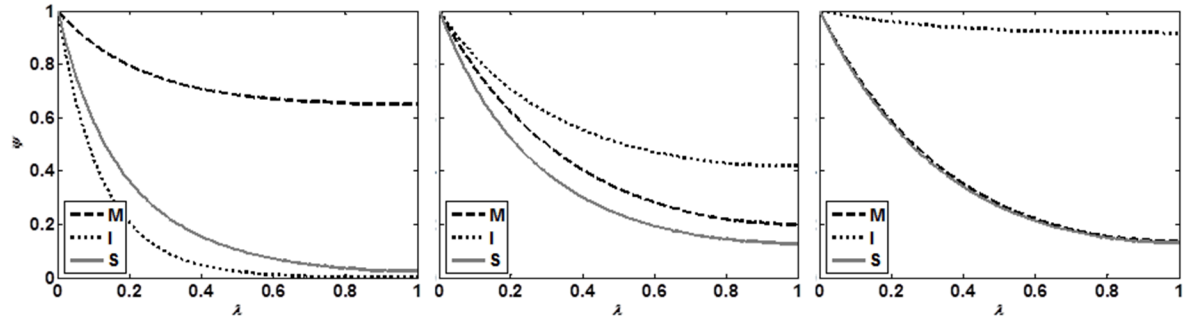
FIGURE 4: Numerical solutions to Eq (3.1-6) in a pore with aspect ratio $L/r = 100$ and a ratio of sticking probabilities (a) $\Gamma_M/\Gamma_I = 0.1$, (b) $\Gamma_M/\Gamma_I = 1$, and (c) $\Gamma_M/\Gamma_I = 10$.
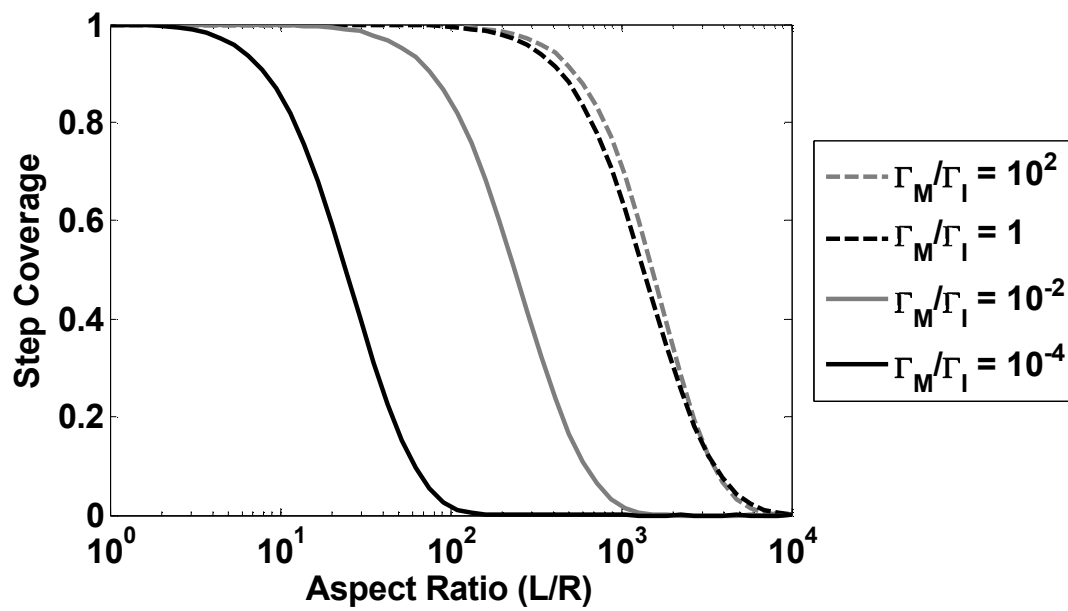
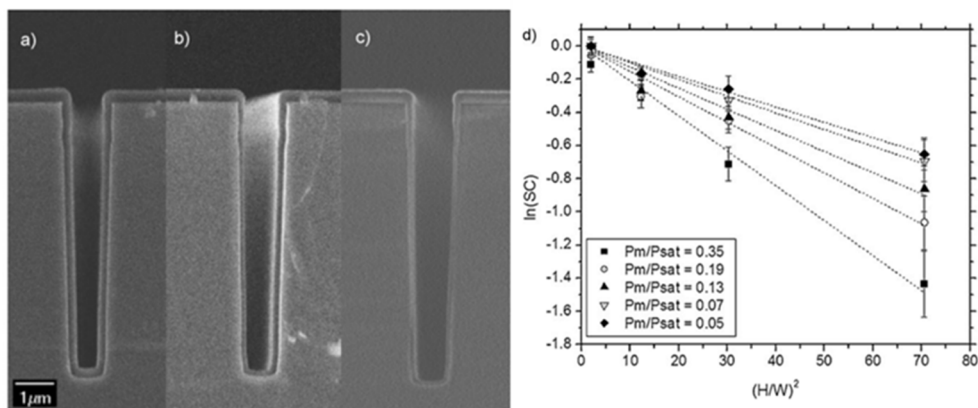**FIGURE 5**: Step coverage S as a function of pore aspect ratio *L/r*, based on numerical solutions to Eq (3.1-6).

FIGURE 6: Films deposited in trenches at P/P^{sat} = (a) 0.05, (b) 0.13, (c) 0.35. Step coverage decreases as P/P^{sat} increases. (d) Fits to Eq (3.2-3); the slopes are used to compute the initiator sticking probability between 0.018 (at P/P^{sat} = 0.05) and 0.043 (at P/P^{sat} = 0.35). Reprinted with permission from [30]. Copyright 2010 Wiley.
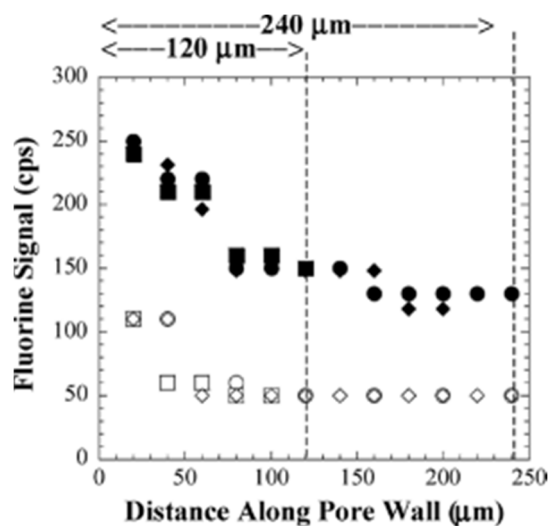
FIGURE 7: Electron microprobe fluorine signal within a membrane pore coated with a fluoropolymer. Unfilled data points were obtained after 2 minutes of coating and filled data points were obtained after 5 minutes of coating. Squares are membrane pores 120 μm deep; diamonds and circles are membrane pores 240 μm deep. Reprinted with permission from [32]. Copyright 2008 American Chemical Society.
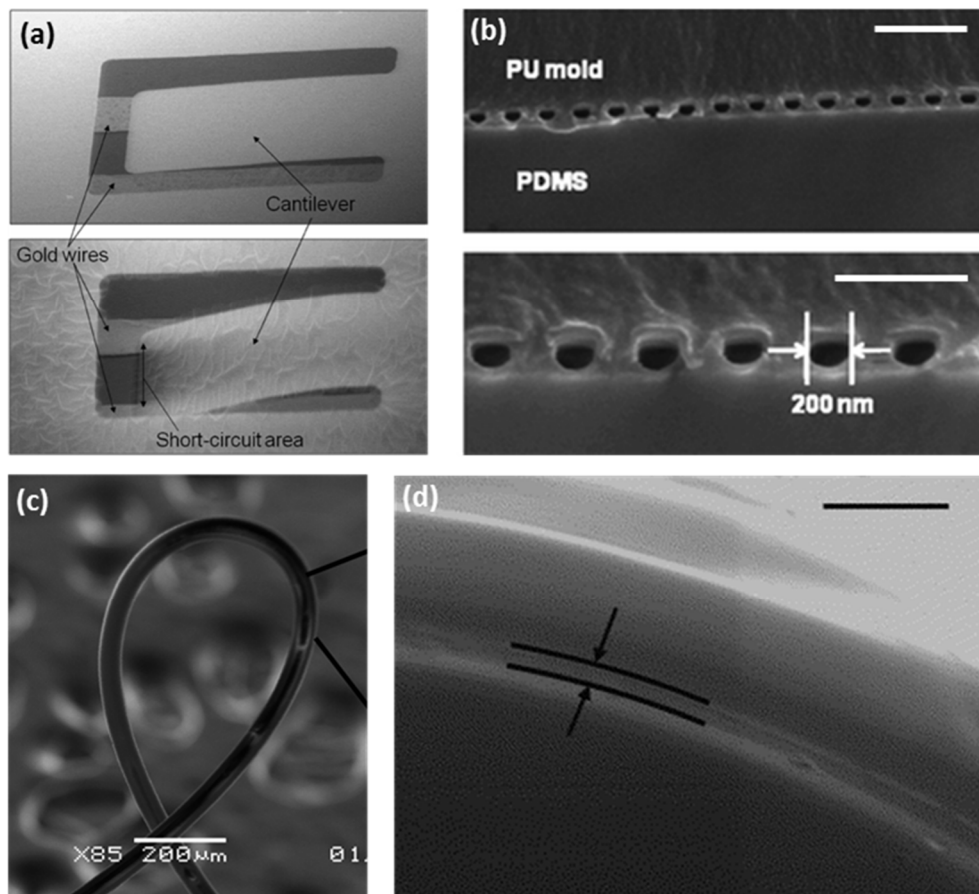
FIGURE 8: (a) 50x20x0.1 μm microcantilever coated with reactive polymer before (top) and after (bottom) reaction with analyte. (b) Microfluidic device with 200 nm wide channels bonded by reaction between coatings on the PU and PDMS pieces. Scale bars represent 1 μm (top) and 500 nm (bottom). (c) Wire coated with flexible, insulating polymer. (d) 195 nm thick anti-microbial coating (between arrows) around a nylon fiber. A layer of carbon is deposited over the nylon-coating assembly for imaging purposes; scale bar represents 1 μm. Reprinted/adapted with permission from (a) [42], copyright 2009 IEEE (b) [43], copyright 2008 Royal Society of Chemistry (c) [50], copyright 2007 American Chemical Society, (d) [53], copyright 2007 Elsevier.